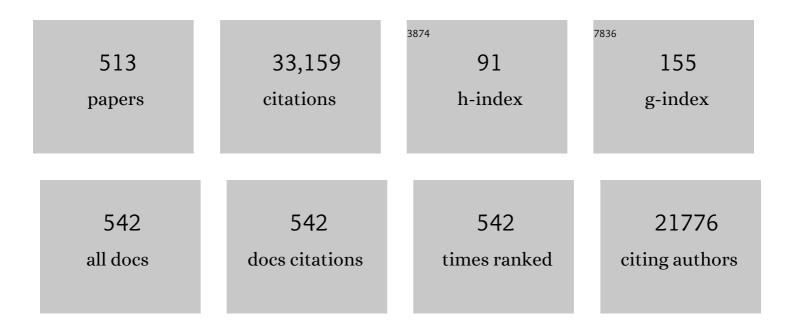
List of Publications by Year in descending order

Source: https://exaly.com/author-pdf/1665865/publications.pdf Version: 2024-02-01



HONG HE

#	Article	IF	CITATIONS
1	Insight into the remarkable enhancement of NH3-SCR performance of Ce-Sn oxide catalyst by tungsten modification. Catalysis Today, 2023, 410, 36-44.	2.2	10
2	Formaldehyde oxidation on Pd/USY catalysts at room temperature: The effect of acid pretreatment on supports. Journal of Environmental Sciences, 2023, 125, 811-822.	3.2	8
3	Atmospheric heterogeneous reactions on soot: A review. Fundamental Research, 2023, 3, 579-591.	1.6	7
4	Advances in emission control of diesel vehicles in China. Journal of Environmental Sciences, 2023, 123, 15-29.	3.2	30
5	Regulating the chemical state of silver via surface hydroxyl groups to enhance ozone decomposition performance of Ag/Fe2O3 catalyst. Catalysis Today, 2023, 410, 117-126.	2.2	3
6	Application of smog chambers in atmospheric process studies. National Science Review, 2022, 9, nwab103.	4.6	21
7	Nano-sized Ag rather than single-atom Ag determines CO oxidation activity and stability. Nano Research, 2022, 15, 452-456.	5.8	35
8	Effects of SO2 on standard and fast SCR over CeWO : A quantitative study of the reaction pathway and active sites. Applied Catalysis B: Environmental, 2022, 301, 120784.	10.8	24
9	Influence of NO on the activity of Pd/ \hat{l} -Al2O3 catalyst for methane oxidation: Alleviation of transient deactivation. Journal of Environmental Sciences, 2022, 112, 38-47.	3.2	5
10	Annual nonmethane hydrocarbon trends in Beijing from 2000 to 2019. Journal of Environmental Sciences, 2022, 112, 210-217.	3.2	14
11	Distinct photocatalytic charges separation pathway on CuOx modified rutile and anatase TiO2 under visible light. Applied Catalysis B: Environmental, 2022, 300, 120735.	10.8	14
12	Unravelling the Mechanism of Intermediateâ€Temperature CO ₂ Interaction with Moltenâ€NaNO ₃ â€Saltâ€Promoted MgO. Advanced Materials, 2022, 34, e2106677.	11.1	21
13	A simple strategy to tune α-MnO2 and enhance VOC oxidation via precipitation rate control. Applied Surface Science, 2022, 576, 151823.	3.1	10
14	Molecular Composition of Oxygenated Organic Molecules and Their Contributions to Organic Aerosol in Beijing. Environmental Science & amp; Technology, 2022, 56, 770-778.	4.6	16
15	Coordinated Control of Fine-Particle and Ozone Pollution by the Substantial Reduction of Nitrogen Oxides. Engineering, 2022, 15, 13-16.	3.2	5
16	A New Type of Quartz Smog Chamber: Design and Characterization. Environmental Science & Technology, 2022, 56, 2181-2190.	4.6	7
17	CeO2 doping boosted low-temperature NH3-SCR activity of FeTiOx catalyst: A microstructure analysis and reaction mechanistic study. Frontiers of Environmental Science and Engineering, 2022, 16, 1.	3.3	5
18	One-pot synthesis of hierarchical MnCu-SSZ-13 catalyst with excellent NH3-SCR activity at low temperatures. Microporous and Mesoporous Materials, 2022, 333, 111720.	2.2	12

#	Article	IF	CITATIONS
19	N-nitration of secondary aliphatic amines in the particle phase. Chemosphere, 2022, 293, 133639.	4.2	6
20	Ceria–tungsten–tin oxide catalysts with superior regeneration capacity after sulfur poisoning for NH ₃ -SCR process. Catalysis Science and Technology, 2022, 12, 2471-2481.	2.1	10
21	Dynamic Change of Active Sites of Supported Vanadia Catalysts for Selective Catalytic Reduction of Nitrogen Oxides. Environmental Science & Technology, 2022, 56, 3710-3718.	4.6	21
22	Generation and Release of OH Radicals from the Reaction of H ₂ O with O ₂ over Soot. Angewandte Chemie - International Edition, 2022, 61, .	7.2	12
23	Low-Temperature SCR Catalyst Development and Industrial Applications in China. Catalysts, 2022, 12, 341.	1.6	15
24	Developing a thermally stable Co/Ce-Sn catalyst via adding Sn for soot and CO oxidation. IScience, 2022, 25, 104103.	1.9	4
25	Dramatic decrease of secondary organic aerosol formation potential in Beijing: Important contribution from reduction of coal combustion emission. Science of the Total Environment, 2022, 832, 155045.	3.9	7
26	Mesoporous LaCoO3 perovskite oxide with high catalytic performance for NO storage and reduction. Journal of Hazardous Materials, 2022, 431, 128528.	6.5	12
27	Layered Double Hydroxide Catalysts for Ozone Decomposition: The Synergic Role of M ²⁺ and M ³⁺ . Environmental Science & Technology, 2022, 56, 1386-1394.	4.6	21
28	Promotion Effect of the Keggin Structure on the Sulfur and Water Resistance of Pt/CeTi Catalysts for CO Oxidation. Catalysts, 2022, 12, 4.	1.6	6
29	Innentitelbild: Generation and Release of OH Radicals from the Reaction of H ₂ O with O ₂ over Soot (Angew. Chem. 21/2022). Angewandte Chemie, 2022, 134, .	1.6	1
30	Influence of photochemical loss of volatile organic compounds on understanding ozone formation mechanism. Atmospheric Chemistry and Physics, 2022, 22, 4841-4851.	1.9	26
31	Hydrothermal Aging Treatment Activates V ₂ O ₅ /TiO ₂ Catalysts for NO _{<i>x</i>} Abatement. Environmental Science & Technology, 2022, 56, 9744-9750.	4.6	23
32	Improved and Reduced Performance of Cu- and Ni-Substituted Co ₃ O ₄ Catalysts with Varying Co _{Oh} /Co _{Td} and Co ³⁺ /Co ²⁺ Ratios for the Complete Catalytic Oxidation of VOCs. Environmental Science & Technology, 2022, 56, 9751-9761.	4.6	31
33	Enhanced Selective Hydrogenolysis of Phenolic C–O Bonds over Graphene-Covered Fe–Co Alloy Catalysts. ACS Sustainable Chemistry and Engineering, 2022, 10, 8588-8596.	3.2	2
34	Effect of Hydroxyl Groups on Metal Anchoring and Formaldehyde Oxidation Performance of Pt/Al ₂ O ₃ . Environmental Science & Technology, 2022, 56, 10916-10924.	4.6	30
35	Theory and practice of metal oxide catalyst design for the selective catalytic reduction of NO with NH3. Catalysis Today, 2021, 376, 292-301.	2.2	71
36	Enhancement of low-temperature NH3-SCR catalytic activity and H2O & SO2 resistance over commercial V2O5-MoO3/TiO2 catalyst by high shear-induced doping of expanded graphite. Catalysis Today, 2021, 376, 302-310.	2.2	44

#	Article	IF	CITATIONS
37	Significant concurrent decrease in PM2.5 and NO2 concentrations in China during COVID-19 epidemic. Journal of Environmental Sciences, 2021, 99, 346-353.	3.2	126
38	In-situ DRIFT assessment on strengthening effect of cerium over FeO /TiO2 catalyst for selective catalytic reduction of NO with NH3. Journal of Rare Earths, 2021, 39, 526-531.	2.5	16
39	Co-function mechanism of multiple active sites over Ag/TiO2 for formaldehyde oxidation. Applied Catalysis B: Environmental, 2021, 282, 119543.	10.8	38
40	A simple strategy to improve Pd dispersion and enhance Pd/TiO2 catalytic activity for formaldehyde oxidation: The roles of surface defects. Applied Catalysis B: Environmental, 2021, 282, 119540.	10.8	117
41	Single atom Fe in favor of carbon disulfide (CS2) adsorption and thus the removal efficiency. Separation and Purification Technology, 2021, 258, 118086.	3.9	28
42	Investigation of suitable precursors for manganese oxide catalysts in ethyl acetate oxidation. Journal of Environmental Sciences, 2021, 104, 17-26.	3.2	10
43	A robust H-transfer redox mechanism determines the high-efficiency catalytic performance of layered double hydroxides. Applied Catalysis B: Environmental, 2021, 285, 119806.	10.8	21
44	Use of rare earth elements in single-atom site catalysis: A critical review — CommemoratingÂtheÂ100thÂanniversaryÂofÂtheAbirthÂofÂAcademicianÂGuangxianÂXu. Journal of Rare Earths, 2021, 39, 233-242.	2.5	28
45	Significant promotion effect of the rutile phase on V ₂ O ₅ /TiO ₂ catalysts for NH ₃ -SCR. Chemical Communications, 2021, 57, 355-358.	2.2	18
46	Surface oxygen species essential for the catalytic activity of Ce–M–Sn (M = Mn or Fe) in soot oxidation. Catalysis Science and Technology, 2021, 11, 895-903.	2.1	12
47	Synergistic Effects of Multicomponents Produce Outstanding Soot Oxidation Activity in a Cs/Co/MnO <i>_x</i> Catalyst. Environmental Science & Technology, 2021, 55, 240-248.	4.6	35
48	A Nonoxide Catalyst System Study: Alkali Metal-Promoted Pt/AC Catalyst for Formaldehyde Oxidation at Ambient Temperature. ACS Catalysis, 2021, 11, 456-465.	5.5	60
49	Chemical formation and source apportionment of PM2.5 at an urban site at the southern foot of the Taihang mountains. Journal of Environmental Sciences, 2021, 103, 20-32.	3.2	10
50	Is reducing new particle formation a plausible solution to mitigate particulate air pollution in Beijing and other Chinese megacities?. Faraday Discussions, 2021, 226, 334-347.	1.6	74
51	Selective catalytic reduction of NO <i>x</i> with NH3: opportunities and challenges of Cu-based small-pore zeolites. National Science Review, 2021, 8, nwab010.	4.6	137
52	Particle growth with photochemical age from new particle formation to haze in the winter of Beijing, China. Science of the Total Environment, 2021, 753, 142207.	3.9	21
53	Iron-Based Composite Oxide Catalysts Tuned by CTAB Exhibit Superior NH3–SCR Performance. Catalysts, 2021, 11, 224.	1.6	7
54	Measurement report: Effects of photochemical aging on the formation and evolution of summertime secondary aerosol in Beijing. Atmospheric Chemistry and Physics, 2021, 21, 1341-1356.	1.9	18

#	Article	IF	CITATIONS
55	Secondary Organic Aerosol Formation Potential from Ambient Air in Beijing: Effects of Atmospheric Oxidation Capacity at Different Pollution Levels. Environmental Science & Technology, 2021, 55, 4565-4572.	4.6	26
56	Terminal Hydroxyl Groups on Al ₂ O ₃ Supports Influence the Valence State and Dispersity of Ag Nanoparticles: Implications for Ozone Decomposition. ACS Omega, 2021, 6, 10715-10722.	1.6	7
57	Superior Oxidative Dehydrogenation Performance toward NH ₃ Determines the Excellent Low-Temperature NH ₃ -SCR Activity of Mn-Based Catalysts. Environmental Science & Technology, 2021, 55, 6995-7003.	4.6	83
58	Role of silver species in H2-NH3-SCR of NOx over Ag/Al2O3 catalysts: Operando spectroscopy and DFT calculations. Journal of Catalysis, 2021, 395, 1-9.	3.1	29
59	The Synergistic Role of Sulfuric Acid, Bases, and Oxidized Organics Governing Newâ€Particle Formation in Beijing. Geophysical Research Letters, 2021, 48, e2020GL091944.	1.5	53
60	Unraveling the Mechanism of Ammonia Selective Catalytic Oxidation on Ag/Al ₂ O ₃ Catalysts by Operando Spectroscopy. ACS Catalysis, 2021, 11, 5506-5516.	5.5	42
61	Investigation into the Enhanced Catalytic Oxidation of <i>o</i> -Xylene over MOF-Derived Co ₃ O ₄ with Different Shapes: The Role of Surface Twofold-Coordinate Lattice Oxygen (O _{2f}). ACS Catalysis, 2021, 11, 6614-6625.	5.5	106
62	Increased primary and secondary H ₂ SO ₄ showing the opposing roles in secondary organic aerosol formation from ethyl methacrylate ozonolysis. Atmospheric Chemistry and Physics, 2021, 21, 7099-7112.	1.9	1
63	Cesium as a dual function promoter in Co/Ce-Sn catalyst for soot oxidation. Applied Catalysis B: Environmental, 2021, 285, 119850.	10.8	32
64	Reaction Pathways of the Selective Catalytic Reduction of NO with NH ₃ on the α-Fe ₂ O ₃ (012) Surface: a Combined Experimental and DFT Study. Environmental Science & Technology, 2021, 55, 10967-10974.	4.6	48
65	Significant contribution of spring northwest transport to volatile organic compounds in Beijing. Journal of Environmental Sciences, 2021, 104, 169-181.	3.2	20
66	Comprehensive Study about the Photolysis of Nitrates on Mineral Oxides. Environmental Science & Technology, 2021, 55, 8604-8612.	4.6	25
67	Effect of relative humidity on SOA formation from aromatic hydrocarbons: Implications from the evolution of gas- and particle-phase species. Science of the Total Environment, 2021, 773, 145015.	3.9	34
68	Design of High-Performance Iron–Niobium Composite Oxide Catalysts for NH ₃ -SCR: Insights into the Interaction between Fe and Nb. ACS Catalysis, 2021, 11, 9825-9836.	5.5	66
69	Adsorption-Induced Active Vanadium Species Facilitate Excellent Performance in Low-Temperature Catalytic NO _{<i>x</i>} Abatement. Journal of the American Chemical Society, 2021, 143, 10454-10461.	6.6	64
70	Promotion Effects of Barium and Cobalt on Manganese Oxide Catalysts for Soot Oxidation. Industrial & Engineering Chemistry Research, 2021, 60, 11412-11420.	1.8	4
71	Mechanistic Study of the Aqueous Reaction of Organic Peroxides with HSO 3 â^ on the Surface of a Water Droplet. Angewandte Chemie, 2021, 133, 20362-20365.	1.6	2
72	Facile homogeneous precipitation method to prepare MnO2 with high performance in catalytic oxidation of ethyl acetate. Chemical Engineering Journal, 2021, 417, 129246.	6.6	35

#	Article	IF	CITATIONS
73	Introducing tin to develop ternary metal oxides with excellent hydrothermal stability for NH3 selective catalytic reduction of NO. Applied Catalysis B: Environmental, 2021, 291, 120125.	10.8	24
74	Mechanistic Study of the Aqueous Reaction of Organic Peroxides with HSO ₃ ^{â^'} on the Surface of a Water Droplet. Angewandte Chemie - International Edition, 2021, 60, 20200-20203.	7.2	9
75	Ozone and SOA formation potential based on photochemical loss of VOCs during the Beijing summer. Environmental Pollution, 2021, 285, 117444.	3.7	75
76	Ammonium nitrate promotes sulfate formation through uptake kinetic regime. Atmospheric Chemistry and Physics, 2021, 21, 13269-13286.	1.9	24
77	Unexpected increase in low-temperature NH3-SCR catalytic activity over Cu-SSZ-39 after hydrothermal aging. Applied Catalysis B: Environmental, 2021, 294, 120237.	10.8	40
78	To enhance water resistance for catalytic ozone decomposition by fabricating H2O adsorption-site in OMS-2 tunnels. Applied Catalysis B: Environmental, 2021, 297, 120466.	10.8	32
79	Redox and acid properties of MnV2Ox/TiO2 catalysts synthesized by assistance of microwave for NO selective catalytic reduction by ammonia. Chemical Engineering Journal Advances, 2021, 8, 100156.	2.4	3
80	Microkinetic study of NO oxidation, standard and fast NH3-SCR on CeWO at low temperatures. Chemical Engineering Journal, 2021, 423, 130128.	6.6	34
81	Highly efficient Ru/CeO ₂ catalysts for formaldehyde oxidation at low temperature and the mechanistic study. Catalysis Science and Technology, 2021, 11, 1914-1921.	2.1	20
82	Improving the representation of HONO chemistry in CMAQ and examining its impact on haze over China. Atmospheric Chemistry and Physics, 2021, 21, 15809-15826.	1.9	21
83	Photochemical Aging of Atmospheric Fine Particles as a Potential Source for Gas-Phase Hydrogen Peroxide. Environmental Science & Technology, 2021, 55, 15063-15071.	4.6	8
84	Boosting the Dispersity of Metallic Ag Nanoparticles and Ozone Decomposition Performance of Ag-Mn Catalysts via Manganese Vacancy-Dependent Metal–Support Interactions. Environmental Science & Technology, 2021, 55, 16143-16152.	4.6	24
85	Tuning Metal–Support Interaction of Pt-CeO ₂ Catalysts for Enhanced Oxidation Reactivity. Environmental Science & Technology, 2021, 55, 16687-16698.	4.6	35
86	Reaction Pathways of Standard and Fast Selective Catalytic Reduction over Cu-SSZ-39. Environmental Science & Technology, 2021, 55, 16175-16183.	4.6	24
87	Cocatalyst Modification of AgTaO ₃ Photocatalyst for Conversion of Carbon Dioxide with Water. Journal of Physical Chemistry C, 2021, 125, 26389-26397.	1.5	7
88	Promotional Effects of Sm/Ce/La Doping on Soot Oxidation over MnCo ₂ O ₄ Spinel Catalysts. Journal of Physical Chemistry C, 2021, 125, 26484-26491.	1.5	7
89	A superior catalyst for ozone decomposition: NiFe layered double hydroxide. Journal of Environmental Sciences, 2021, , .	3.2	1
90	Tuning the fill percentage in the hydrothermal synthesis process to increase catalyst performance for ozone decomposition. Journal of Environmental Sciences, 2020, 87, 60-70.	3.2	13

#	Article	IF	CITATIONS
91	Effect of support preparation with different concentration precipitant on the NO storage performance of Pt/BaO/CeO2 catalysts. Catalysis Today, 2020, 339, 135-147.	2.2	14
92	A superior Fe-V-Ti catalyst with high activity and SO2 resistance for the selective catalytic reduction of NO with NH3. Journal of Hazardous Materials, 2020, 382, 120970.	6.5	95
93	The way to enhance the thermal stability of V2O5-based catalysts for NH3-SCR. Catalysis Today, 2020, 355, 408-414.	2.2	23
94	Promoting effect of microwave irradiation on CeO2-TiO2 catalyst for selective catalytic reduction of NO by NH3. Journal of Rare Earths, 2020, 38, 59-69.	2.5	37
95	Effects of SO ₂ on Cu-SSZ-39 catalyst for the selective catalytic reduction of NO _x with NH ₃ . Catalysis Science and Technology, 2020, 10, 1256-1263.	2.1	39
96	Effects of SO2 and H2O on low-temperature NO conversion over F-V2O5-WO3/TiO2 catalysts. Journal of Environmental Sciences, 2020, 90, 253-261.	3.2	22
97	Detrimental role of residual surface acid ions on ozone decomposition over Ce-modified Î ³ -MnO2 under humid conditions. Journal of Environmental Sciences, 2020, 91, 43-53.	3.2	34
98	Promotion effect of cerium doping on iron–titanium composite oxide catalysts for selective catalytic reduction of NO _x with NH ₃ . Catalysis Science and Technology, 2020, 10, 648-657.	2.1	26
99	Novel CeMnaOx catalyst for highly efficient catalytic decomposition of ozone. Applied Catalysis B: Environmental, 2020, 264, 118498.	10.8	47
100	Effect of treatment atmosphere on the vanadium species of V/TiO ₂ catalysts for the selective catalytic reduction of NO _x with NH ₃ . Catalysis Science and Technology, 2020, 10, 311-314.	2.1	16
101	Synthesis of Cu-SSZ-13 catalyst by using different silica sources for NO-SCR by NH3. Molecular Catalysis, 2020, 484, 110738.	1.0	8
102	A comparative study of the activity and hydrothermal stability of Al-rich Cu-SSZ-39 and Cu-SSZ-13. Applied Catalysis B: Environmental, 2020, 264, 118511.	10.8	143
103	Influence of atmospheric conditions on sulfuric acid-dimethylamine-ammonia-based new particle formation. Chemosphere, 2020, 245, 125554.	4.2	30
104	Enhancing Oxygen Vacancies of Ce-OMS-2 via Optimized Hydrothermal Conditions to Improve Catalytic Ozone Decomposition. Industrial & Engineering Chemistry Research, 2020, 59, 118-128.	1.8	32
105	Catalysis and Nanomaterials for Sustainable Energy, Environment, and Industry: Special Issue for World Chemistry Forum 2019, Barcelona, Spain. Topics in Catalysis, 2020, 63, 777-777.	1.3	0
106	Unprecedented Ambient Sulfur Trioxide (SO ₃) Detection: Possible Formation Mechanism and Atmospheric Implications. Environmental Science and Technology Letters, 2020, 7, 809-818.	3.9	34
107	Distinct NO ₂ Effects on Cu-SSZ-13 and Cu-SSZ-39 in the Selective Catalytic Reduction of NO _{<i>x</i>} with NH ₃ . Environmental Science & Technology, 2020, 54, 15499-15506.	4.6	48
108	Passive NO Adsorption on Hydrothermally Aged Pd-Based Small-Pore Zeolites. Topics in Catalysis, 2020, 63, 944-953.	1.3	19

#	Article	IF	CITATIONS
109	Effects of alkali and alkaline earth metals on Cu-SSZ-39 catalyst for the selective catalytic reduction of NO with NH3. Chemical Engineering Journal, 2020, 388, 124250.	6.6	49
110	Air Pollutant Correlations in China: Secondary Air Pollutant Responses to NO _{<i>x</i>} and SO ₂ Control. Environmental Science and Technology Letters, 2020, 7, 695-700.	3.9	113
111	Insights into Designing Photocatalysts for Gaseous Ammonia Oxidation under Visible Light. Environmental Science & Technology, 2020, 54, 10544-10550.	4.6	22
112	Identification of a Facile Pathway for Dioxymethylene Conversion to Formate Catalyzed by Surface Hydroxyl on TiO ₂ -Based Catalyst. ACS Catalysis, 2020, 10, 9706-9715.	5.5	82
113	Understanding the knowledge gaps between air pollution controls and health impacts including pathogen epidemic. Environmental Research, 2020, 189, 109949.	3.7	23
114	Single-atom site catalysts for environmental catalysis. Nano Research, 2020, 13, 3165-3182.	5.8	252
115	Combination of Low- and Medium-Temperature Catalysts for the Selective Catalytic Reduction of NOx with NH3. Topics in Catalysis, 2020, 63, 924-931.	1.3	8
116	Continuous and comprehensive atmospheric observations in Beijing: a station to understand the complex urban atmospheric environment. Big Earth Data, 2020, 4, 295-321.	2.0	54
117	Efficient Conversion of NO to NO ₂ on SO ₂ -Aged MgO under Atmospheric Conditions. Environmental Science & Technology, 2020, 54, 11848-11856.	4.6	15
118	Recent advances in three-way catalysts of natural gas vehicles. Catalysis Science and Technology, 2020, 10, 6407-6419.	2.1	55
119	Improving the catalytic performance of ozone decomposition over Pd-Ce-OMS-2 catalysts under harsh conditions. Catalysis Science and Technology, 2020, 10, 7671-7680.	2.1	19
120	Tuning the Chemical State of Silver on Ag–Mn Catalysts to Enhance the Ozone Decomposition Performance. Environmental Science & Technology, 2020, 54, 11566-11575.	4.6	31
121	Formaldehyde Oxidation on Pd/TiO2 Catalysts at Room Temperature: The Effects of Surface Oxygen Vacancies. Topics in Catalysis, 2020, 63, 810-816.	1.3	16
122	Recent Progress on Improving Low-Temperature Activity of Vanadia-Based Catalysts for the Selective Catalytic Reduction of NOx with Ammonia. Catalysts, 2020, 10, 1421.	1.6	27
123	Promoting Effect of Mn on In Situ Synthesized Cu-SSZ-13 for NH3-SCR. Catalysts, 2020, 10, 1375.	1.6	12
124	Importance of controllable Al sites in CHA framework by crystallization pathways for NH3-SCR reaction. Applied Catalysis B: Environmental, 2020, 277, 119193.	10.8	43
125	Challenges and opportunities for manganese oxides in low-temperature selective catalytic reduction of NOx with NH3: H2O resistance ability. Journal of Solid State Chemistry, 2020, 289, 121464.	1.4	42
126	Recent advances in catalytic decomposition of ozone. Journal of Environmental Sciences, 2020, 94, 14-31.	3.2	93

#	Article	IF	CITATIONS
127	Investigation of Suitable Templates for One-Pot-Synthesized Cu-SAPO-34 in NO _{<i>x</i>} Abatement from Diesel Vehicle Exhaust. Environmental Science & Technology, 2020, 54, 7870-7878.	4.6	37
128	Role of dimethyl ether in incipient soot formation in premixed ethylene flames. Combustion and Flame, 2020, 216, 271-279.	2.8	24
129	Inhibitory role of excessive NH3 in NH3-SCR on CeWOx at low temperatures. Catalysis Science and Technology, 2020, 10, 2758-2762.	2.1	4
130	A MnO2-based catalyst with H2O resistance for NH3-SCR: Study of catalytic activity and reactants-H2O competitive adsorption. Applied Catalysis B: Environmental, 2020, 270, 118860.	10.8	159
131	Contrasting trends of PM2.5 and surface-ozone concentrations in China from 2013 to 2017. National Science Review, 2020, 7, 1331-1339.	4.6	284
132	Hydrothermal Stability Enhancement of Al-Rich Cu-SSZ-13 for NH ₃ Selective Catalytic Reduction Reaction by Ion Exchange with Cerium and Samarium. Industrial & Engineering Chemistry Research, 2020, 59, 6416-6423.	1.8	29
133	High-performance of Cu-TiO2 for photocatalytic oxidation of formaldehyde under visible light and the mechanism study. Chemical Engineering Journal, 2020, 390, 124481.	6.6	91
134	Impacts of Mixed Gaseous and Particulate Pollutants on Secondary Particle Formation during Ozonolysis of Butyl Vinyl Ether. Environmental Science & Technology, 2020, 54, 3909-3919.	4.6	4
135	The adsorption and oxidation of SO ₂ on MgO surface: experimental and DFT calculation studies. Environmental Science: Nano, 2020, 7, 1092-1101.	2.2	18
136	Quantitative determination of the Cu species, acid sites and NH ₃ -SCR mechanism on Cu-SSZ-13 and H-SSZ-13 at low temperatures. Catalysis Science and Technology, 2020, 10, 1135-1150.	2.1	16
137	Resolving the puzzle of single-atom silver dispersion on nanosized Î ³ -Al2O3 surface for high catalytic performance. Nature Communications, 2020, 11, 529.	5.8	111
138	Precise control of post-treatment significantly increases hydrothermal stability of in-situ synthesized cu-zeolites for NH3-SCR reaction. Applied Catalysis B: Environmental, 2020, 266, 118655.	10.8	88
139	Chemical characterization of submicron aerosol in summertime Beijing: A case study in southern suburbs in 2018. Chemosphere, 2020, 247, 125918.	4.2	17
140	Effect of SO2 treatment in the presence and absence of O2 over ceria–titania oxides for selective catalytic reduction. Journal of Materials Science, 2020, 55, 4570-4577.	1.7	3
141	Adsorptive removal of toluene and dichloromethane from humid exhaust on MFI, BEA and FAU zeolites: An experimental and theoretical study. Chemical Engineering Journal, 2020, 394, 124986.	6.6	58
142	The effect of crystallite size on low-temperature hydrothermal stability of Cu-SAPO-34. Catalysis Science and Technology, 2020, 10, 2855-2863.	2.1	16
143	Water Promotes the Oxidation of SO ₂ by O ₂ over Carbonaceous Aerosols. Environmental Science & Technology, 2020, 54, 7070-7077.	4.6	28
144	Investigation of the common intermediates over Fe-ZSM-5 in NH3-SCR reaction at low temperature by in situ DRIFTS. Journal of Environmental Sciences, 2020, 94, 32-39.	3.2	27

#	Article	IF	CITATIONS
145	Hydrothermal aging alleviates the inhibition effects of NO2 on Cu-SSZ-13 for NH3-SCR. Applied Catalysis B: Environmental, 2020, 275, 119105.	10.8	71
146	Investigation of Water and Sulfur Tolerance of Precipitable Silver Compound Ag/Al ₂ O ₃ Catalysts in H ₂ -Assisted C ₃ H ₆ -SCR of NO <i>x</i> . ACS Omega, 2020, 5, 29593-29600.	1.6	10
147	Interfacial structure-governed SO ₂ resistance of Cu/TiO ₂ catalysts in the catalytic oxidation of CO. Catalysis Science and Technology, 2020, 10, 1661-1674.	2.1	20
148	Industrial carbon dioxide capture and utilization: state of the art and future challenges. Chemical Society Reviews, 2020, 49, 8584-8686.	18.7	610
149	The promotion effect of nitrous acid on aerosol formation in wintertime in Beijing: the possible contribution of traffic-related emissions. Atmospheric Chemistry and Physics, 2020, 20, 13023-13040.	1.9	37
150	Shape-controlled synthesis of Pd nanocrystals with exposed {110} facets and their catalytic applications. Catalysis Today, 2019, 327, 28-36.	2.2	37
151	Shape dependence of support for NO storage and reduction catalysts. Journal of Environmental Sciences, 2019, 75, 396-407.	3.2	6
152	Variations and sources of nitrous acid (HONO) during a severe pollution episode in Beijing in winter 2016. Science of the Total Environment, 2019, 648, 253-262.	3.9	62
153	High Pt utilization efficiency of electrocatalysts for oxygen reduction reaction in alkaline media. Catalysis Today, 2019, 332, 101-108.	2.2	28
154	Experimental and DFT study of the adsorption of N2O on transition ion-exchanged ZSM-5. Catalysis Today, 2019, 327, 177-181.	2.2	23
155	The effects of H ₂ O on a vanadium-based catalyst for NH ₃ -SCR at low temperatures: a quantitative study of the reaction pathway and active sites. Catalysis Science and Technology, 2019, 9, 5593-5604.	2.1	11
156	Nanodispersed Mn ₃ O ₄ /γ-Al ₂ O ₃ for NO ₂ Elimination at Room Temperature. Environmental Science & Technology, 2019, 53, 10855-10862.	4.6	15
157	Role of Structural Defects in MnO _{<i>x</i>} Promoted by Ag Doping in the Catalytic Combustion of Volatile Organic Compounds and Ambient Decomposition of O ₃ . Environmental Science & Technology, 2019, 53, 10871-10879.	4.6	100
158	Oxidation Potential Reduction of Carbon Nanomaterials during Atmospheric-Relevant Aging: Role of Surface Coating. Environmental Science & Technology, 2019, 53, 10454-10461.	4.6	13
159	The effect of water on the heterogeneous reactions of SO ₂ and NH ₃ on the surfaces of α-Fe ₂ O ₃ and γ-Al ₂ O ₃ . Environmental Science: Nano, 2019, 6, 2749-2758.	2.2	30
160	Impacts of SO ₂ , Relative Humidity, and Seed Acidity on Secondary Organic Aerosol Formation in the Ozonolysis of Butyl Vinyl Ether. Environmental Science & Technology, 2019, 53, 8845-8853.	4.6	22
161	Influence of functional groups on toxicity of carbon nanomaterials. Atmospheric Chemistry and Physics, 2019, 19, 8175-8187.	1.9	32
162	A review of experimental techniques for aerosol hygroscopicity studies. Atmospheric Chemistry and Physics, 2019, 19, 12631-12686.	1.9	80

#	Article	IF	CITATIONS
163	Mechanism of the H ₂ Effect on NH ₃ -Selective Catalytic Reduction over Ag/Al ₂ O ₃ : Kinetic and Diffuse Reflectance Infrared Fourier Transform Spectroscopy Studies. ACS Catalysis, 2019, 9, 10489-10498.	5.5	28
164	Theoretical Study of PAH Growth by Phenylacetylene Addition. Journal of Physical Chemistry A, 2019, 123, 10323-10332.	1.1	8
165	Activity enhancement of Pt/MnO _x catalyst by novel β-MnO ₂ for low-temperature CO oxidation: study of the CO–O ₂ competitive adsorption and active oxygen species. Catalysis Science and Technology, 2019, 9, 347-354.	2.1	33
166	Cu-exchanged RTH-type zeolites for NH ₃ -selective catalytic reduction of NO _x : Cu distribution and hydrothermal stability. Catalysis Science and Technology, 2019, 9, 106-115.	2.1	35
167	Contrary Role of H ₂ O and O ₂ in the Kinetics of Heterogeneous Photochemical Reactions of SO ₂ on TiO ₂ . Journal of Physical Chemistry A, 2019, 123, 1311-1318.	1.1	26
168	Important role of aromatic hydrocarbons in SOA formation from unburned gasoline vapor. Atmospheric Environment, 2019, 201, 101-109.	1.9	33
169	Acidic permanganate oxidation of sulfamethoxazole by stepwise electron-proton transfer. Chemosphere, 2019, 222, 71-82.	4.2	16
170	Significant source of secondary aerosol: formation from gasoline evaporative emissions in the presence of SO ₂ and NH ₃ . Atmospheric Chemistry and Physics, 2019, 19, 8063-8081.	1.9	52
171	Effects of ultrasonic treatment on dithiothreitol (DTT) assay measurements for carbon materials. Journal of Environmental Sciences, 2019, 84, 51-58.	3.2	7
172	Enhancement of aqueous sulfate formation by the coexistence of NO2/NH3 under high ionic strengths in aerosol water. Environmental Pollution, 2019, 252, 236-244.	3.7	49
173	A Comprehensive Study about the Hygroscopic Behavior of Mixtures of Oxalic Acid and Nitrate Salts: Implication for the Occurrence of Atmospheric Metal Oxalate Complex. ACS Earth and Space Chemistry, 2019, 3, 1216-1225.	1.2	16
174	Effect of Organic Assistant on the Performance of Ceria-Based Catalysts for the Selective Catalytic Reduction of NO with Ammonia. Catalysts, 2019, 9, 357.	1.6	8
175	Atomic-scale insights into zeolite-based catalysis in N2O decomposition. Science of the Total Environment, 2019, 673, 266-271.	3.9	15
176	SSZ-13 Synthesized by Solvent-Free Method: A Potential Candidate for NH ₃ -SCR Catalyst with High Activity and Hydrothermal Stability. Industrial & Engineering Chemistry Research, 2019, 58, 5397-5403.	1.8	23
177	Secondary organic aerosol formation from the OH-initiated oxidation of guaiacol under different experimental conditions. Atmospheric Environment, 2019, 207, 30-37.	1.9	27
178	Water adsorption and hygroscopic growth of six anemophilous pollen species: the effect of temperature. Atmospheric Chemistry and Physics, 2019, 19, 2247-2258.	1.9	35
179	Polytetrafluoroethylene modifying: A low cost and easy way to improve the H2O resistance ability over MnOx for low-temperature NH3-SCR. Journal of Environmental Chemical Engineering, 2019, 7, 103044.	3.3	26
180	Improvement of low-temperature catalytic activity over hierarchical Fe-Beta catalysts for selective catalytic reduction of NO with NH3. Chinese Chemical Letters, 2019, 30, 867-870.	4.8	31

#	Article	IF	CITATIONS
181	Parameterization of heterogeneous reaction of SO2 to sulfate on dust with coexistence of NH3 and NO2 under different humidity conditions. Atmospheric Environment, 2019, 208, 133-140.	1.9	37
182	Significant enhancement in water resistance of Pd/Al2O3 catalyst for benzene oxidation by Na addition. Chinese Chemical Letters, 2019, 30, 1450-1454.	4.8	26
183	Rate constant and secondary organic aerosol formation from the gas-phase reaction of eugenol with hydroxyl radicals. Atmospheric Chemistry and Physics, 2019, 19, 2001-2013.	1.9	20
184	Enhancement of secondary organic aerosol formation and its oxidation state by SO ₂ during photooxidation of 2-methoxyphenol. Atmospheric Chemistry and Physics, 2019, 19, 2687-2700.	1.9	22
185	The promotional effect of H2 reduction treatment on the low-temperature NH3-SCR activity of Cu/SAPO-18. Applied Surface Science, 2019, 483, 536-544.	3.1	32
186	Drivers of improved PM _{2.5} air quality in China from 2013 to 2017. Proceedings of the National Academy of Sciences of the United States of America, 2019, 116, 24463-24469.	3.3	1,193
187	Effects of NO ₂ and C ₃ H ₆ on the heterogeneous oxidation of SO ₂ on TiO ₂ in the presence or absence of UV–Vis irradiation.	1.9	21
188	Atmospheric Chemistry and Physics, 2019, 19, 19, 19, 2019. The ammonia synthesis reaction on A mini-review on the role of quasi-compounds in catalysis — The ammonia synthesis reaction on metals. Surface Science, 2019, 679, 264-272.	0.8	5
189	Quantitative study of the NH3-SCR pathway and the active site distribution over CeWO at low temperatures. Journal of Catalysis, 2019, 369, 372-381.	3.1	53
190	The balance of acidity and redox capability over modified CeO2 catalyst for the selective catalytic reduction of NO with NH3. Journal of Environmental Sciences, 2019, 79, 273-279.	3.2	34
191	A laboratory study on the hygroscopic behavior of H2C2O4-containing mixed particles. Atmospheric Environment, 2019, 200, 34-39.	1.9	7
192	Facile synthesis of Ag-modified manganese oxide for effective catalytic ozone decomposition. Journal of Environmental Sciences, 2019, 80, 159-168.	3.2	38
193	Electrochemical oxidation of gaseous benzene on a Sb-SnO2/foam Ti nano-coating electrode in all-solid cell. Chemosphere, 2019, 217, 780-789.	4.2	16
194	Insights into the Activation Effect of H ₂ Pretreatment on Ag/Al ₂ O ₃ Catalyst for the Selective Oxidation of Ammonia. ACS Catalysis, 2019, 9, 1437-1445.	5.5	78
195	Differences of the oxidation process and secondary organic aerosol formation at low and high precursor concentrations. Journal of Environmental Sciences, 2019, 79, 256-263.	3.2	29
196	Insight into the origin of sulfur tolerance of Ag/Al2O3 in the H2-C3H6-SCR of NOx. Applied Catalysis B: Environmental, 2019, 244, 909-918.	10.8	46
197	Deactivation of Cu-SSZ-13 in the presence of SO2 during hydrothermal aging. Catalysis Today, 2019, 320, 84-90.	2.2	62
198	Promoting Effect of Organic Ligand on the Performance of Ceria for the Selective Catalytic Reduction of NO by NH ₃ . ChemistrySelect, 2018, 3, 2683-2691.	0.7	6

#	Article	IF	CITATIONS
199	The smart surface modification of Fe2O3 by WO for significantly promoting the selective catalytic reduction of NO with NH3. Applied Catalysis B: Environmental, 2018, 230, 165-176.	10.8	182
200	The Keggin Structure: An Important Factor in Governing NH3–SCR Activity Over the V2O5–MoO3/TiO2 Catalyst. Catalysis Letters, 2018, 148, 1228-1235.	1.4	22
201	Alkali resistance promotion of Ce-doped vanadium-titanic-based NH3-SCR catalysts. Journal of Environmental Sciences, 2018, 73, 155-161.	3.2	31
202	Nanosize Effect of Al ₂ O ₃ in Ag/Al ₂ O ₃ Catalyst for the Selective Catalytic Oxidation of Ammonia. ACS Catalysis, 2018, 8, 2670-2682.	5.5	144
203	A Low-Temperature Route Triggered by Water Vapor during the Ethanol-SCR of NO <i>x</i> over Ag/Al ₂ O ₃ . ACS Catalysis, 2018, 8, 2699-2708.	5.5	28
204	Precisely controlled synthesis of α-/β-MnO ₂ materials by adding Zn(acac) ₂ as a phase transformation-inducing agent. Chemical Communications, 2018, 54, 1477-1480.	2.2	16
205	Silver Valence State Determines the Water Tolerance of Ag/Al ₂ O ₃ for the H ₂ –C ₃ H ₆ –SCR of NO <i>_x</i> . Journal of Physical Chemistry C, 2018, 122, 670-680.	1.5	20
206	Palladium supported on low-surface-area fiber-based materials for catalytic oxidation of volatile organic compounds. Chemical Engineering Journal, 2018, 348, 361-369.	6.6	58
207	Role of Carbonaceous Aerosols in Catalyzing Sulfate Formation. ACS Catalysis, 2018, 8, 3825-3832.	5.5	59
208	Facet-dependent performance of anatase TiO2 for photocatalytic oxidation of gaseous ammonia. Applied Catalysis B: Environmental, 2018, 223, 209-215.	10.8	65
209	Insight into the Role of Pd State on Pdâ€Based Catalysts in <i>o</i> â€Xylene Oxidation at Low Temperature. ChemCatChem, 2018, 10, 998-1004.	1.8	28
210	Response of soil methane uptake to simulated nitrogen deposition and grazing management across three types of steppe in Inner Mongolia, China. Science of the Total Environment, 2018, 612, 799-808.	3.9	14
211	NO promotion of SO2 conversion to sulfate: An important mechanism for the occurrence of heavy haze during winter in Beijing. Environmental Pollution, 2018, 233, 662-669.	3.7	82
212	Specific Role of Potassium in Promoting Ag/Al ₂ O ₃ for Catalytic Oxidation of Formaldehyde at Low Temperature. Journal of Physical Chemistry C, 2018, 122, 27331-27339.	1.5	53
213	Polymeric vanadyl species determine the low-temperature activity of V-based catalysts for the SCR of NO _{<i>x</i>} with NH ₃ . Science Advances, 2018, 4, eaau4637.	4.7	206
214	A CeO2/ZrO2-TiO2 Catalyst for the Selective Catalytic Reduction of NOx with NH3. Catalysts, 2018, 8, 592.	1.6	18
215	Molecular Insights into NO-Promoted Sulfate Formation on Model TiO ₂ Nanoparticles with Different Exposed Facets. Environmental Science & amp; Technology, 2018, 52, 14110-14118.	4.6	19
216	Oxygen Vacancies Induced by Transition Metal Doping in γ-MnO ₂ for Highly Efficient Ozone Decomposition. Environmental Science & Technology, 2018, 52, 12685-12696.	4.6	236

#	Article	IF	CITATIONS
217	Effects of NO ₂ Addition on the NH ₃ -SCR over Small-Pore Cu–SSZ-13 Zeolites with Varying Cu Loadings. Journal of Physical Chemistry C, 2018, 122, 25948-25953.	1.5	58
218	Sodium Enhances Ir/TiO ₂ Activity for Catalytic Oxidation of Formaldehyde at Ambient Temperature. ACS Catalysis, 2018, 8, 11377-11385.	5.5	102
219	Selective Catalytic Reduction of NOx. Catalysts, 2018, 8, 459.	1.6	22
220	Hydrothermal Stability of CeO2–WO3–ZrO2 Mixed Oxides for Selective Catalytic Reduction of NOx by NH3. Environmental Science & Technology, 2018, 52, 11769-11777.	4.6	24
221	Morphology-Dependent Catalytic Performance of NbO _{<i>x</i>} /CeO ₂ Catalysts for Selective Catalytic Reduction of NO _{<i>x</i>} with NH ₃ . Industrial & amp; Engineering Chemistry Research, 2018, 57, 12736-12741.	1.8	43
222	Secondary Organic Aerosol Formation from Ambient Air at an Urban Site in Beijing: Effects of OH Exposure and Precursor Concentrations. Environmental Science & Technology, 2018, 52, 6834-6841.	4.6	42
223	Electrochemical oxidation of volatile organic compounds in all-solid cell at ambient temperature. Chemical Engineering Journal, 2018, 354, 93-104.	6.6	13
224	DRIFT Study on Promotion Effect of the Keggin Structure over V2O5-MoO3/TiO2 Catalysts for Low Temperature NH3-SCR Reaction. Catalysts, 2018, 8, 143.	1.6	24
225	Silver incorporated into cryptomelane-type Manganese oxide boosts the catalytic oxidation of benzene. Applied Catalysis B: Environmental, 2018, 239, 214-222.	10.8	111
226	Role of NH ₃ in the Heterogeneous Formation of Secondary Inorganic Aerosols on Mineral Oxides. Journal of Physical Chemistry A, 2018, 122, 6311-6320.	1.1	25
227	Synergistic Effect of TiO ₂ –SiO ₂ in Ag/Si–Ti Catalyst for the Selective Catalytic Oxidation of Ammonia. Industrial & Engineering Chemistry Research, 2018, 57, 11903-11910.	1.8	42
228	Influence of metal-mediated aerosol-phase oxidation on secondary organic aerosol formation from the ozonolysis and OH-oxidation of α-pinene. Scientific Reports, 2017, 7, 40311.	1.6	15
229	Activity of Selective Catalytic Reduction of NO over V2O5/TiO2 Catalysts Preferentially Exposed Anatase {001} and {101} Facets. Catalysis Letters, 2017, 147, 934-945.	1.4	26
230	Remarkable synergistic effect between {001} facets and surface F ions promoting hole migration on anatase TiO2. Applied Catalysis B: Environmental, 2017, 207, 397-403.	10.8	50
231	SO ₂ Initiates the Efficient Conversion of NO ₂ to HONO on MgO Surface. Environmental Science & Technology, 2017, 51, 3767-3775.	4.6	76
232	An alumina-supported silver catalyst with high water tolerance for H2 assisted C3H6-SCR of NOx. Applied Catalysis B: Environmental, 2017, 207, 60-71.	10.8	45
233	Effects of SO2 on the low temperature selective catalytic reduction of NO by NH3 over CeO2-V2O5-WO3/TiO2 catalysts. Frontiers of Environmental Science and Engineering, 2017, 11, 1.	3.3	12
234	Enhanced Oxidation of Tetracycline by Permanganate via the Alkali-Induced Alteration of the Highest Occupied Molecular Orbital and the Electrostatic Potential. Industrial & Engineering Chemistry Research, 2017, 56, 4703-4708.	1.8	12

#	Article	IF	CITATIONS
235	High temperature reduction dramatically promotes Pd/TiO2 catalyst for ambient formaldehyde oxidation. Applied Catalysis B: Environmental, 2017, 217, 560-569.	10.8	167
236	Improvement of Nb Doping on SO ₂ Resistance of VO _{<i>x</i>} /CeO ₂ Catalyst for the Selective Catalytic Reduction of NO _{<i>x</i>} with NH ₃ . Journal of Physical Chemistry C, 2017, 121, 7803-7809.	1.5	53
237	Hydrogen production from oxidative steam reforming of ethanol over Ir catalysts supported on Ce–La solid solution. International Journal of Hydrogen Energy, 2017, 42, 11177-11186.	3.8	11
238	Heterogeneous reaction of SO2 with soot: The roles of relative humidity and surface composition of soot in surface sulfate formation. Atmospheric Environment, 2017, 152, 465-476.	1.9	68
239	Structure–activity relationship of surface hydroxyl groups during NO ₂ adsorption and transformation on TiO ₂ nanoparticles. Environmental Science: Nano, 2017, 4, 2388-2394.	2.2	49
240	Oxygen vacancy clusters essential for the catalytic activity of CeO2 nanocubes for o-xylene oxidation. Scientific Reports, 2017, 7, 12845.	1.6	75
241	New Insight into and Characterization of the Aqueous Metal-Enol(ate) Complexes of (Acetonedicarboxylato)copper. ACS Omega, 2017, 2, 6728-6740.	1.6	3
242	Heterogeneous reaction of NO2 with soot at different relative humidity. Environmental Science and Pollution Research, 2017, 24, 21248-21255.	2.7	15
243	Complete oxidation of formaldehyde at room temperature over an Al-rich Beta zeolite supported platinum catalyst. Applied Catalysis B: Environmental, 2017, 219, 200-208.	10.8	65
244	Heterogeneous Reaction of SO2 on Manganese Oxides: the Effect of Crystal Structure and Relative Humidity. Scientific Reports, 2017, 7, 4550.	1.6	56
245	Significant enhancement in activity of Pd/TiO 2 catalyst for formaldehyde oxidation by Na addition. Catalysis Today, 2017, 281, 412-417.	2.2	50
246	Transition metal doped cryptomelane-type manganese oxide catalysts for ozone decomposition. Applied Catalysis B: Environmental, 2017, 201, 503-510.	10.8	238
247	Effect of V ₂ O ₅ Additive on the SO ₂ Resistance of a Fe ₂ O ₃ /AC Catalyst for NH ₃ -SCR of NO _{<i>x</i>} at Low Temperatures. Industrial & Engineering Chemistry Research, 2016, 55, 2677-2685.	1.8	75
248	A novel W-doped Ni-Mg mixed oxide catalyst for CO2 methanation. Applied Catalysis B: Environmental, 2016, 196, 108-116.	10.8	155
249	Effect of Doping Metals on OMS-2/γ-Al ₂ O ₃ Catalysts for Plasma-Catalytic Removal of <i>o</i> -Xylene. Journal of Physical Chemistry C, 2016, 120, 6136-6144.	1.5	40
250	A novel one-pot synthesized CuCe-SAPO-34 catalyst with high NH3-SCR activity and H2O resistance. Catalysis Communications, 2016, 81, 20-23.	1.6	38
251	Influence of sulfur in fuel on the properties of diffusion flame soot. Atmospheric Environment, 2016, 142, 383-392.	1.9	17
252	Water Effect on Preparation of Ag/Al ₂ O ₃ Catalyst for Reduction of NOx by Ethanol. Journal of Physical Chemistry C, 2016, 120, 24294-24301.	1.5	18

#	Article	IF	CITATIONS
253	Ozonolysis of Trimethylamine Exchanged with Typical Ammonium Salts in the Particle Phase. Environmental Science & Technology, 2016, 50, 11076-11084.	4.6	18
254	The photoenhanced aging process of soot by the heterogeneous ozonization reaction. Physical Chemistry Chemical Physics, 2016, 18, 24401-24407.	1.3	23
255	DFT studies on the heterogeneous oxidation of SO ₂ by oxygen functional groups on graphene. Physical Chemistry Chemical Physics, 2016, 18, 31691-31697.	1.3	39
256	Synergetic formation of secondary inorganic and organic aerosol: effect of SO ₂ and NH ₃ on particle formation and growth. Atmospheric Chemistry and Physics, 2016, 16, 14219-14230.	1.9	102
257	High-resolution ammonia emissions inventories in China from 1980 to 2012. Atmospheric Chemistry and Physics, 2016, 16, 2043-2058.	1.9	281
258	Promotion of ceria for decomposition of ammonia bisulfate over V2O5-MoO3/TiO2 catalyst for selective catalytic reduction. Chemical Engineering Journal, 2016, 303, 275-281.	6.6	84
259	Resistance to SO2 poisoning of V2O5/TiO2-PILC catalyst for the selective catalytic reduction of NO by NH3. Chinese Journal of Catalysis, 2016, 37, 888-897.	6.9	27
260	Oxygen vacancies on nanosized ceria govern the NO _x storage capacity of NSR catalysts. Catalysis Science and Technology, 2016, 6, 3950-3962.	2.1	50
261	Nitrogen deposition but not climate warming promotes Deyeuxia angustifolia encroachment in alpine tundra of the Changbai Mountains, Northeast China. Science of the Total Environment, 2016, 544, 85-93.	3.9	21
262	Exploring the nitrous acid (HONO) formation mechanism in winter Beijing: direct emissions and heterogeneous production in urban and suburban areas. Faraday Discussions, 2016, 189, 213-230.	1.6	77
263	Effects of precursors for manganese-loaded γ-Al2O3 catalysts on plasma-catalytic removal of o-xylene. Chemical Engineering Journal, 2016, 288, 406-413.	6.6	48
264	Distinct potential aerosol masses under different scenarios of transport at a suburban site of Beijing. Journal of Environmental Sciences, 2016, 39, 52-61.	3.2	13
265	Shape dependence of nanoceria on complete catalytic oxidation of o-xylene. Catalysis Science and Technology, 2016, 6, 4840-4848.	2.1	62
266	High hydrothermal stability of Cu–SAPO-34 catalysts for the NH3-SCR of NOx. Chemical Engineering Journal, 2016, 294, 254-263.	6.6	121
267	Synergistic formation of sulfate and ammonium resulting from reaction between SO ₂ and NH ₃ on typical mineral dust. Physical Chemistry Chemical Physics, 2016, 18, 956-964.	1.3	66
268	Influence of alkali metals on Pd/TiO ₂ catalysts for catalytic oxidation of formaldehyde at room temperature. Catalysis Science and Technology, 2016, 6, 2289-2295.	2.1	107
269	Enhanced photocatalytic oxidation of NO over g-C3N4-TiO2 under UV and visible light. Applied Catalysis B: Environmental, 2016, 184, 28-34.	10.8	304
270	Antimicrobial activity of silver loaded MnO2 nanomaterials with different crystal phases against Escherichia coli. Journal of Environmental Sciences, 2016, 41, 112-120.	3.2	24

#	Article	IF	CITATIONS
271	Promotional effect of Nb additive on the activity and hydrothermal stability for the selective catalytic reduction of NO with NH3 over CeZrO catalyst. Applied Catalysis B: Environmental, 2016, 180, 766-774.	10.8	158
272	Effect of Support on the Activity of Ag-based Catalysts for Formaldehyde Oxidation. Scientific Reports, 2015, 5, 12950.	1.6	86
273	Complete Catalytic Oxidation of Ethanol over MnO ₂ with Different Crystal Phase Structures. Wuli Huaxue Xuebao/ Acta Physico - Chimica Sinica, 2015, 31, 353-359.	2.2	7
274	Laboratory study on OH-initiated degradation kinetics of dehydroabietic acid. Physical Chemistry Chemical Physics, 2015, 17, 10953-10962.	1.3	14
275	Role of ammonia in forming secondary aerosols from gasoline vehicle exhaust. Science China Chemistry, 2015, 58, 1377-1384.	4.2	35
276	Catalytic oxidation of CO on metals involving an ionic process in the presence of H2O: the role of promoting materials. RSC Advances, 2015, 5, 949-959.	1.7	13
277	Discerning the Role of Ag–O–Al Entities on Ag/γ-Al ₂ O ₃ Surface in NOx Selective Reduction by Ethanol. Journal of Physical Chemistry C, 2015, 119, 3132-3142.	1.5	28
278	Catalytic oxidation of formaldehyde over manganese oxides with different crystal structures. Catalysis Science and Technology, 2015, 5, 2305-2313.	2.1	464
279	Effect of aluminium dust on secondary organic aerosol formation in m-xylene/NO x photo-oxidation. Science China Earth Sciences, 2015, 58, 245-254.	2.3	8
280	Secondary aerosol formation and oxidation capacity in photooxidation in the presence of Al2O3 seed particles and SO2. Science China Chemistry, 2015, 58, 1426-1434.	4.2	14
281	Remarkable promotion effect of trace sulfation on OMS-2 nanorod catalysts for the catalytic combustion of ethanol. Journal of Environmental Sciences, 2015, 35, 69-75.	3.2	18
282	Comparisons of measured nitrous acid (HONO) concentrations in a pollution period at urban and suburban Beijing, in autumn of 2014. Science China Chemistry, 2015, 58, 1393-1402.	4.2	41
283	Heterogeneous Kinetics of <i>cis</i> -Pinonic Acid with Hydroxyl Radical under Different Environmental Conditions. Journal of Physical Chemistry A, 2015, 119, 6583-6593.	1.1	22
284	The effect of Fe species distribution and acidity of Fe-ZSM-5 on the hydrothermal stability and SO2 and hydrocarbons durability in NH3-SCR reaction. Chinese Journal of Catalysis, 2015, 36, 649-656.	6.9	39
285	Significant Promotion Effect of Mo Additive on a Novel Ce–Zr Mixed Oxide Catalyst for the Selective Catalytic Reduction of NO _{<i>x</i>} with NH ₃ . ACS Applied Materials & Interfaces, 2015, 7, 9497-9506.	4.0	186
286	Nb-doped VO _x /CeO ₂ catalyst for NH ₃ -SCR of NO _x at low temperatures. RSC Advances, 2015, 5, 37675-37681.	1.7	33
287	Effects of post-treatment method and Na co-cation on the hydrothermal stability of Cu–SSZ-13 catalyst for the selective catalytic reduction of NO with NH3. Applied Catalysis B: Environmental, 2015, 179, 206-212.	10.8	105
288	DRIFTS study of a Ce–W mixed oxide catalyst for the selective catalytic reduction of NOx with NH3. Catalysis Science and Technology, 2015, 5, 2290-2299.	2.1	74

#	Article	IF	CITATIONS
289	The role of Ag O Al entities in adsorption of NCO species and reduction of NO. Catalysis Today, 2015, 258, 35-40.	2.2	4
290	Effect of Fe on the photocatalytic removal of NO over visible light responsive Fe/TiO2 catalysts. Applied Catalysis B: Environmental, 2015, 179, 21-28.	10.8	124
291	Influence of relative humidity on heterogeneous kinetics of NO ₂ on kaolin and hematite. Physical Chemistry Chemical Physics, 2015, 17, 19424-19431.	1.3	43
292	Adsorption states of typical intermediates on Ag/Al2O3 catalyst employed in the selective catalytic reduction of NOx by ethanol. Chinese Journal of Catalysis, 2015, 36, 1312-1320.	6.9	10
293	The Effects of Mn ²⁺ Precursors on the Structure and Ozone Decomposition Activity of Cryptomelane-Type Manganese Oxide (OMS-2) Catalysts. Journal of Physical Chemistry C, 2015, 119, 23119-23126.	1.5	144
294	Promotion Effect of H ₂ on Ethanol Oxidation and NO _{<i>x</i>} Reduction with Ethanol over Ag/Al ₂ O ₃ Catalyst. Environmental Science & Technology, 2015, 49, 481-488.	4.6	31
295	Ordered mesoporous and bulk Co3O4 supported Pd catalysts for catalytic oxidation of o-xylene. Catalysis Today, 2015, 242, 294-299.	2.2	58
296	Decomposition of high-level ozone under high humidity over Mn–Fe catalyst: The influence of iron precursors. Catalysis Communications, 2015, 59, 156-160.	1.6	103
297	High-efficiency reduction of NO emission from diesel exhaust using a CeWO catalyst. Catalysis Communications, 2015, 59, 226-228.	1.6	36
298	Effect of preparation methods on the activity of VO _x /CeO ₂ catalysts for the selective catalytic reduction of NO _x with NH ₃ . Catalysis Science and Technology, 2015, 5, 389-396.	2.1	37
299	Environmentally-benign catalysts for the selective catalytic reduction of NO _x from diesel engines: structure–activity relationship and reaction mechanism aspects. Chemical Communications, 2014, 50, 8445-8463.	2.2	248
300	Enhanced Activity of Ti-Modified V ₂ O ₅ /CeO ₂ Catalyst for the Selective Catalytic Reduction of NO _{<i>x</i>} with NH ₃ . Industrial & Engineering Chemistry Research, 2014, 53, 19506-19511.	1.8	88
301	Role of aggregated Fe oxo species in N2O decomposition over Fe/ZSM-5. Chinese Journal of Catalysis, 2014, 35, 1972-1981.	6.9	9
302	Hygroscopicity of particles generated from photooxidation of α-pinene under different oxidation conditions in the presence of sulfate seed aerosols. Journal of Environmental Sciences, 2014, 26, 129-139.	3.2	10
303	Haze insights and mitigation in China: An overview. Journal of Environmental Sciences, 2014, 26, 2-12.	3.2	91
304	Photocatalytic oxidation of gaseous ammonia over fluorinated TiO2 with exposed (001) facets. Applied Catalysis B: Environmental, 2014, 152-153, 82-87.	10.8	56
305	Morphology-dependent bactericidal activities of Ag/CeO2 catalysts against Escherichia coli. Journal of Inorganic Biochemistry, 2014, 135, 45-53.	1.5	83

306 Synthesis and herbicidal activities of 2-methylpropan-2-aminium O-methyl 1-(substituted) Tj ETQq0 0 0 rgBT /Overlock 10 Tf 50 62 Td (p

#	Article	IF	CITATIONS
307	Degradation kinetics of levoglucosan initiated by hydroxyl radical under different environmental conditions. Atmospheric Environment, 2014, 91, 32-39.	1.9	129
308	Excellent antimicrobial properties of silver-loaded mesoporous silica SBA-15. Journal of Applied Microbiology, 2014, 116, 1106-1118.	1.4	23
309	A common feature of H ₂ -assisted HC-SCR over Ag/Al ₂ O ₃ . Catalysis Science and Technology, 2014, 4, 1239-1245.	2.1	21
310	Mineral dust and NOx promote the conversion of SO2 to sulfate in heavy pollution days. Scientific Reports, 2014, 4, 4172.	1.6	426
311	Inhibitory effect of NO2 on the selective catalytic reduction of NOx with NH3 over one-pot-synthesized Cu–SSZ-13 catalyst. Catalysis Science and Technology, 2014, 4, 1104.	2.1	119
312	Nature of Ag Species on Ag/γ-Al ₂ O ₃ : A Combined Experimental and Theoretical Study. ACS Catalysis, 2014, 4, 2776-2784.	5.5	64
313	Effect of sulfur poisoning on Co3O4/CeO2 composite oxide catalyst for soot combustion. Chinese Journal of Catalysis, 2014, 35, 1504-1510.	6.9	12
314	Sodium-Promoted Pd/TiO ₂ for Catalytic Oxidation of Formaldehyde at Ambient Temperature. Environmental Science & Technology, 2014, 48, 5816-5822.	4.6	253
315	Selective catalytic reduction of NOx by NH3 for heavy-duty diesel vehicles. Chinese Journal of Catalysis, 2014, 35, 1438-1445.	6.9	19
316	NOx selective catalytic reduction by ammonia over Cu-ETS-10 catalysts. Chinese Journal of Catalysis, 2014, 35, 1030-1035.	6.9	13
317	Decreasing effect and mechanism of FeSO 4 seed particles on secondary organic aerosol in α -pinene photooxidation. Environmental Pollution, 2014, 193, 88-93.	3.7	27
318	Photocatalytic Removal of NO _{<i>x</i>} over Visible Light Responsive Oxygen-Deficient TiO ₂ . Journal of Physical Chemistry C, 2014, 118, 7434-7441.	1.5	116
319	Excellent Performance of One-Pot Synthesized Cu-SSZ-13 Catalyst for the Selective Catalytic Reduction of NO _{<i>x</i>} with NH ₃ . Environmental Science & Technology, 2014, 48, 566-572.	4.6	264
320	The use of ceria for the selective catalytic reduction of NOx with NH3. Chinese Journal of Catalysis, 2014, 35, 1251-1259.	6.9	121
321	Manganese–niobium mixed oxide catalyst for the selective catalytic reduction of NOx with NH3 at low temperatures. Chemical Engineering Journal, 2014, 250, 390-398.	6.6	238
322	Effect of TiO2 calcination temperature on the photocatalytic oxidation of gaseous NH3. Journal of Environmental Sciences, 2014, 26, 673-682.	3.2	30
323	Fabrication of nanofibrous A- or B-sites substituted LaCoO3 perovskites with macroscopic structures and their catalytic applications. Materials Research Bulletin, 2014, 51, 295-301.	2.7	8
324	Research Progress in Vanadium-Free Catalysts for the Selective Catalytic Re-duction of NO with NH3. Chinese Journal of Catalysis, 2014, 32, 1113-1128.	6.9	4

#	Article	IF	CITATIONS
325	The abatement of major pollutants in air and water by environmental catalysis. Frontiers of Environmental Science and Engineering, 2013, 7, 302-325.	3.3	37
326	Novel MnWOx catalyst with remarkable performance for low temperature NH3-SCR of NOx. Catalysis Science and Technology, 2013, 3, 2699.	2.1	140
327	Effect of mineral dust on secondary organic aerosol yield and aerosol size in α-pinene/NOx photo-oxidation. Atmospheric Environment, 2013, 77, 781-789.	1.9	35
328	Highly dispersed iron vanadate catalyst supported on TiO2 for the selective catalytic reduction of NOx with NH3. Journal of Catalysis, 2013, 307, 340-351.	3.1	149
329	Heterogeneous photochemical reaction of ozone with anthracene adsorbed on mineral dust. Atmospheric Environment, 2013, 72, 165-170.	1.9	15
330	Heterogeneous and multiphase formation pathways of gypsum in the atmosphere. Physical Chemistry Chemical Physics, 2013, 15, 19196.	1.3	25
331	Laboratory Study on the Hygroscopic Behavior of External and Internal C ₂ –C ₄ Dicarboxylic Acid–NaCl Mixtures. Environmental Science & Technology, 2013, 47, 130827153621004.	4.6	27
332	Heterogeneous photochemical aging of soot by NO2 under simulated sunlight. Atmospheric Environment, 2013, 64, 270-276.	1.9	50
333	An XAFS study on the specific microstructure of active species in iron titanate catalyst for NH3-SCR of NOx. Catalysis Today, 2013, 201, 131-138.	2.2	25
334	Activation of solid surface as catalyst. Catalysis Today, 2013, 201, 2-6.	2.2	6
335	Effect of pretreatment on Pd/Al2O3 catalyst for catalytic oxidation of o-xylene at low temperature. Journal of Environmental Sciences, 2013, 25, 1206-1212.	3.2	50
336	Hydrogen production from oxidative steam reforming of ethanol over rhodium catalysts supported on Ce–La solid solution. International Journal of Hydrogen Energy, 2013, 38, 10293-10304.	3.8	47
337	Fuel reforming over Ni-based catalysts coupled with selective catalytic reduction of NOx. Chinese Journal of Catalysis, 2013, 34, 1407-1417.	6.9	5
338	A cyclic reaction pathway triggered by ammonia for the selective catalytic reduction of NOx by ethanol over Ag/Al2O3. Applied Catalysis B: Environmental, 2013, 136-137, 103-111.	10.8	30
339	Review of heterogeneous photochemical reactions of NOy on aerosol — A possible daytime source of nitrous acid (HONO) in the atmosphere. Journal of Environmental Sciences, 2013, 25, 326-334.	3.2	36
340	Oxidative steam reforming of ethanol over Rh catalyst supported on Ce1â^'xLaxOy (xÂ=Â0.3) solid solution prepared by urea co-precipitation method. Journal of Power Sources, 2013, 238, 57-64.	4.0	33
341	Low CO content hydrogen production from oxidative steam reforming of ethanol over CuO-CeO2 catalysts at low-temperature. Journal of Energy Chemistry, 2013, 22, 861-868.	7.1	19
342	Magnetic core–shell Fe3O4@C-SO3H nanoparticle catalyst for hydrolysis of cellulose. Cellulose, 2013, 20, 127-134.	2.4	81

#	Article	IF	CITATIONS
343	Well-dispersed palladium supported on ordered mesoporous Co3O4 for catalytic oxidation of o-xylene. Applied Catalysis B: Environmental, 2013, 142-143, 72-79.	10.8	93
344	Hygroscopic properties of oxalic acid and atmospherically relevant oxalates. Atmospheric Environment, 2013, 69, 281-288.	1.9	46
345	NH ₃ -SCR Performance of Fresh and Hydrothermally Aged Fe-ZSM-5 in Standard and Fast Selective Catalytic Reduction Reactions. Environmental Science & amp; Technology, 2013, 47, 3293-3298.	4.6	108
346	Alumina with Various Pore Structures Prepared by Spray Pyrolysis of Inorganic Aluminum Precursors. Industrial & Engineering Chemistry Research, 2013, 52, 13377-13383.	1.8	6
347	Role of Organic Carbon in Heterogeneous Reaction of NO ₂ with Soot. Environmental Science & Technology, 2013, 47, 3174-3181.	4.6	70
348	XAFS Study on the Specific Deoxidation Behavior of Iron Titanate Catalyst for the Selective Catalytic Reduction of NO _{<i>x</i>} with NH ₃ . ChemCatChem, 2013, 5, 3760-3769.	1.8	31
349	Effect of soot microstructure on its ozonization reactivity. Journal of Chemical Physics, 2012, 137, 084507.	1.2	25
350	Differences in the reactivity of ammonium salts with methylamine. Atmospheric Chemistry and Physics, 2012, 12, 4855-4865.	1.9	30
351	Heterogeneous reaction of acetic acid on MgO, α-Al2O3, and CaCO3 and the effect on the hygroscopic behaviour of these particles. Physical Chemistry Chemical Physics, 2012, 14, 8403.	1.3	71
352	Synergistic reaction between SO2 and NO2 on mineraloxides: a potential formation pathway of sulfate aerosol. Physical Chemistry Chemical Physics, 2012, 14, 1668-1676.	1.3	143
353	Heterogeneous Uptake of Amines by Citric Acid and Humic Acid. Environmental Science & Technology, 2012, 46, 11112-11118.	4.6	34
354	Influence of Combustion Conditions on Hydrophilic Properties and Microstructure of Flame Soot. Journal of Physical Chemistry A, 2012, 116, 4129-4136.	1.1	46
355	Intimate contact of enolic species with silver sites benefits the SCR of NOx by ethanol over Ag/Al2O3. Journal of Catalysis, 2012, 293, 13-26.	3.1	47
356	Alkaliâ€Metalâ€Promoted Pt/TiO ₂ Opens a More Efficient Pathway to Formaldehyde Oxidation at Ambient Temperatures. Angewandte Chemie - International Edition, 2012, 51, 9628-9632.	7.2	611
357	Hydrothermal Deactivation of Fe-ZSM-5 Prepared by Different Methods for the Selective Catalytic Reduction of NOx with NH3. Chinese Journal of Catalysis, 2012, 33, 454-464.	6.9	26
358	Key role of organic carbon in the sunlight-enhanced atmospheric aging of soot by O ₂ . Proceedings of the National Academy of Sciences of the United States of America, 2012, 109, 21250-21255.	3.3	66
359	An environmentally-benign CeO2-TiO2 catalyst for the selective catalytic reduction of NO with NH3 in simulated diesel exhaust. Catalysis Today, 2012, 184, 160-165.	2.2	163
360	A superior Ce-W-Ti mixed oxide catalyst for the selective catalytic reduction of NOx with NH3. Applied Catalysis B: Environmental, 2012, 115-116, 100-106.	10.8	562

#	Article	IF	CITATIONS
361	Synergistic effect in the humidifying process of atmospheric relevant calcium nitrate, calcite and oxalic acid mixtures. Atmospheric Environment, 2012, 50, 97-102.	1.9	34
362	A case study of Asian dust storm particles: Chemical composition, reactivity to SO2 and hygroscopic properties. Journal of Environmental Sciences, 2012, 24, 62-71.	3.2	43
363	Glucose production from hydrolysis of cellulose over a novel silica catalyst under hydrothermal conditions. Journal of Environmental Sciences, 2012, 24, 473-478.	3.2	33
364	Effects of Ce on catalytic combustion of methane over Pd-Pt/Al2O3 catalyst. Journal of Environmental Sciences, 2012, 24, 507-511.	3.2	31
365	Environmental-friendly catalysts for the selective catalytic reduction of NO _{<italic>x</italic>} . Scientia Sinica Chimica, 2012, 42, 446-468.	0.2	3
366	Three-dimensionally ordered macroporous Ce0.8Zr0.2O2-supported gold nanoparticles: synthesis with controllable size and super-catalytic performance for soot oxidation. Energy and Environmental Science, 2011, 4, 2959.	15.6	171
367	Novel cerium–tungsten mixed oxide catalyst for the selective catalytic reduction of NOx with NH3. Chemical Communications, 2011, 47, 8046.	2.2	335
368	Facile In-Situ Synthesis of Manganese Dioxide Nanosheets on Cellulose Fibers and their Application in Oxidative Decomposition of Formaldehyde. Journal of Physical Chemistry C, 2011, 115, 16873-16878.	1.5	116
369	Complete catalytic oxidation of o-xylene over CeO2 nanocubes. Journal of Environmental Sciences, 2011, 23, 160-165.	3.2	26
370	Experimental and density functional theory study of the adsorption of N2O on ion-exchanged ZSM-5: Part II. The adsorption of N2O on main-group ion-exchanged ZSM-5. Journal of Environmental Sciences, 2011, 23, 681-686.	3.2	11
371	Influence of coating method on catalyst activity of AgCl/Al2O3/SUS304 composite plate. Journal of Environmental Sciences, 2011, 23, S90-S94.	3.2	0
372	A direct sulfation method for introducing the transition metal cation Co2+ into ZrO2 with little change in the BrA,nsted acid sites. Journal of Catalysis, 2011, 279, 301-309.	3.1	8
373	Heterogeneous reactions between NO2 and anthracene adsorbed on SiO2 and MgO. Atmospheric Environment, 2011, 45, 917-924.	1.9	35
374	Mechanism of the selective catalytic reduction of NOx with NH3 over environmental-friendly iron titanate catalyst. Catalysis Today, 2011, 175, 18-25.	2.2	170
375	Mechanism of highly selective low temperature PROX reaction of CO in H2: Oxidation of CO via HCOO with OH. Catalysis Today, 2011, 175, 467-470.	2.2	29
376	The Remarkable Improvement of a CeTi based Catalyst for NO _{<i>x</i>} Abatement, Prepared by a Homogeneous Precipitation Method. ChemCatChem, 2011, 3, 1286-1289.	1.8	103
377	Effects of Adding CeO2 to Ag/Al2O3 Catalyst for Ammonia Oxidation at Low Temperatures. Chinese Journal of Catalysis, 2011, 32, 727-735.	6.9	22
378	Highly Active Catalysts of Gold Nanoparticles Supported on Threeâ€Dimensionally Ordered Macroporous LaFeO ₃ for Soot Oxidation. Angewandte Chemie - International Edition, 2011, 50, 2326-2329.	7.2	306

#	Article	IF	CITATIONS
379	Influence of calcination temperature on iron titanate catalyst for the selective catalytic reduction of NOx with NH3. Catalysis Today, 2011, 164, 520-527.	2.2	98
380	Influence of sulfation on iron titanate catalyst for the selective catalytic reduction of NOx with NH3. Applied Catalysis B: Environmental, 2011, 103, 369-377.	10.8	245
381	Effects of temperature and reductant type on the process of NOx storage reduction over Pt/Ba/CeO2 catalysts. Applied Catalysis B: Environmental, 2011, 104, 151-160.	10.8	34
382	Heterogeneous reactions of carbonyl sulfide on mineral oxides: mechanism and kinetics study. Atmospheric Chemistry and Physics, 2010, 10, 10335-10344.	1.9	17
383	Flower-like tungsten oxide particles: Synthesis, characterization and dimethyl methylphosphonate sensing properties. Analytica Chimica Acta, 2010, 675, 36-41.	2.6	21
384	Removal of arsenate from water by using an Fe–Ce oxide adsorbent: Effects of coexistent fluoride and phosphate. Journal of Hazardous Materials, 2010, 179, 208-214.	6.5	38
385	A comparative investigation of NdSrCu1â^'xCoxO4â^'Î′ and Sm1.8Ce0.2Cu1â^'xCoxO4â^'Î′ (x: 0–0.4) for NO decomposition. Journal of Environmental Sciences, 2010, 22, 448-453.	3.2	8
386	In situ DRIFTS study of hygroscopic behavior of mineral aerosol. Journal of Environmental Sciences, 2010, 22, 555-560.	3.2	64
387	Removal of bromate ion using powdered activated carbon. Journal of Environmental Sciences, 2010, 22, 1846-1853.	3.2	40
388	Degradation kinetics of anthracene by ozone on mineral oxides. Atmospheric Environment, 2010, 44, 4446-4453.	1.9	36
389	Remarkable influence of reductant structure on the activity of alumina-supported silver catalyst for the selective catalytic reduction of NOx. Journal of Catalysis, 2010, 271, 343-350.	3.1	28
390	Precipitable silver compound catalysts for the selective catalytic reduction of NOx by ethanol. Applied Catalysis A: General, 2010, 375, 258-264.	2.2	54
391	Selective catalytic reduction of NO with NH3 over iron titanate catalyst: Catalytic performance and characterization. Applied Catalysis B: Environmental, 2010, 96, 408-420.	10.8	258
392	Effect of Co addition to Pt/Ba/Al2O3 system for NOx storage and reduction. Applied Catalysis B: Environmental, 2010, 100, 19-30.	10.8	35
393	Ultrasound-assisted nanocasting fabrication and excellent catalytic performance of three-dimensionally ordered mesoporous chromia for the combustion of formaldehyde, acetone, and methanol. Applied Catalysis B: Environmental, 2010, 100, 229-237.	10.8	106
394	Selective catalytic reduction of NO with NH3 over manganese substituted iron titanate catalyst: Reaction mechanism and H2O/SO2 inhibition mechanism study. Catalysis Today, 2010, 153, 70-76.	2.2	183
395	Mesoporous transition alumina with uniform pore structure synthesized by alumisol spray pyrolysis. Chemical Engineering Journal, 2010, 163, 133-142.	6.6	33
396	Heterogeneous uptake of carbonyl sulfide onto kaolinite within a temperature range of 220–330 K. Journal of Geophysical Research, 2010, 115, .	3.3	13

#	Article	IF	CITATIONS
397	Plasmon-Induced Photodegradation of Toxic Pollutants with Agâ^'AgI/Al ₂ O ₃ under Visible-Light Irradiation. Journal of the American Chemical Society, 2010, 132, 857-862.	6.6	541
398	Structureâ^'Activity Relationship of Iron Titanate Catalysts in the Selective Catalytic Reduction of NO _{<i>x</i>} with NH ₃ . Journal of Physical Chemistry C, 2010, 114, 16929-16936.	1.5	304
399	The Utilization of Physisorption Analyzer for Studying the Hygroscopic Properties of Atmospheric Relevant Particles. Journal of Physical Chemistry A, 2010, 114, 4232-4237.	1.1	30
400	Ultrasound-Assisted Nanocasting Fabrication of Ordered Mesoporous MnO ₂ and Co ₃ O ₄ with High Surface Areas and Polycrystalline Walls. Journal of Physical Chemistry C, 2010, 114, 2694-2700.	1.5	108
401	Electrochemical Synthesis of Catalytically Active Ru/RuO ₂ Coreâ^'Shell Nanoparticles without Stabilizer. Chemistry of Materials, 2010, 22, 4056-4061.	3.2	43
402	Structural and hygroscopic changes of soot during heterogeneous reaction with O3. Physical Chemistry Chemical Physics, 2010, 12, 10896.	1.3	86
403	Preparation o fMagnetic Sulfonated Carbon-Based Solid Acid Catalysts for the Hydrolysis of Cellulose. Wuli Huaxue Xuebao/ Acta Physico - Chimica Sinica, 2010, 26, 1873-1878.	2.2	6
404	Advances in Mechanistic and Practical Studies on the Selective Catalytic Reduction of NO _x by Oxygenated Hydrocarbons over Ag/Al ₂ O ₃ . Chinese Journal of Catalysis, 2010, 31, 491-501.	6.9	5
405	The role of silver species on Ag/Al2O3 catalysts for the selective catalytic oxidation of ammonia to nitrogen. Journal of Catalysis, 2009, 261, 101-109.	3.1	126
406	Pretreatments of Co3O4 at moderate temperature for CO oxidation at â^'80 °C. Journal of Catalysis, 2009, 267, 121-128.	3.1	298
407	Mechanism of selective catalytic oxidation of ammonia to nitrogen over Ag/Al2O3. Journal of Catalysis, 2009, 268, 18-25.	3.1	178
408	In situ adsorption-catalysis system for the removal of o-xylene over an activated carbon supported Pd catalyst. Journal of Environmental Sciences, 2009, 21, 985-990.	3.2	36
409	Coating of Î ³ -Al2O3 on the stainless steel substrate by electrophoretic deposition method. Journal of Environmental Sciences, 2009, 21, S112-S115.	3.2	10
410	A CO-Tolerant Hydrogen Fuel Cell System Designed by Combining with an Extremely Active Pt/CNT Catalyst. Catalysis Letters, 2009, 127, 148-151.	1.4	8
411	Effect of the pressure on the catalytic oxidation of volatile organic compounds over Ag/Al2O3 catalyst. Applied Catalysis B: Environmental, 2009, 89, 659-664.	10.8	40
412	Effect of manganese substitution on the structure and activity of iron titanate catalyst for the selective catalytic reduction of NO with NH3. Applied Catalysis B: Environmental, 2009, 93, 194-204.	10.8	579
413	Promotion Effects and Mechanism of Alkali Metals and Alkaline Earth Metals on Cobaltâ^'Cerium Composite Oxide Catalysts for N ₂ O Decomposition. Environmental Science & Technology, 2009, 43, 890-895.	4.6	112
414	Experimental and Theoretical Study of Hydrogen Thiocarbonate for Heterogeneous Reaction of Carbonyl Sulfide on Magnesium Oxide. Journal of Physical Chemistry A, 2009, 113, 3387-3394.	1.1	32

#	Article	IF	CITATIONS
415	Dynamic Characterization of the Intermediates for Low-Temperature PROX Reaction of CO in H ₂ —Oxidation of CO with OH via HCOO Intermediate. Journal of Physical Chemistry C, 2009, 113, 12427-12433.	1.5	63
416	Deactivation of a Ce/TiO ₂ Catalyst by SO ₂ in the Selective Catalytic Reduction of NO by NH ₃ . Journal of Physical Chemistry C, 2009, 113, 4426-4432.	1.5	385
417	Comparative study of the effect of water on the heterogeneous reactions of carbonyl sulfide on the surface of α-Al ₂ 0 ₃ and MgO. Atmospheric Chemistry and Physics, 2009, 9, 6273-6286.	1.9	36
418	Influence of Alkaline Earth Metals on Cobalt-Cerium Composite Oxide Catalysts for N ₂ O Decomposition. Wuli Huaxue Xuebao/ Acta Physico - Chimica Sinica, 2009, 25, 1033-1039.	2.2	6
419	The Mechanism for the Selective Oxidation of CO Enhanced by H2O on a Novel PROC Catalyst. Catalysis Letters, 2008, 120, 210-214.	1.4	20
420	Review of Ag/Al2O3-Reductant System in the Selective Catalytic Reduction of NO x. Catalysis Surveys From Asia, 2008, 12, 38-55.	1.0	56
421	DFT and experimental investigations of the formation and adsorption of enolic species on Al2O3 catalyst. Journal of Molecular Structure, 2008, 892, 320-324.	1.8	1
422	DRIFTS investigation and DFT calculation of the adsorption of CO on Pt/TiO2, Pt/CeO2 and FeOx/Pt/CeO2. Spectrochimica Acta - Part A: Molecular and Biomolecular Spectroscopy, 2008, 71, 1193-1198.	2.0	23
423	Experimental and theoretical studies of surface nitrate species on Ag/Al2O3 using DRIFTS and DFT. Spectrochimica Acta - Part A: Molecular and Biomolecular Spectroscopy, 2008, 71, 1446-1451.	2.0	41
424	Efficient disinfection of Escherichia coli in water by silver loaded alumina. Journal of Inorganic Biochemistry, 2008, 102, 1736-1742.	1.5	43
425	Complete oxidation of o-xylene over Pd/Al2O3 catalyst at low temperature. Catalysis Today, 2008, 139, 15-23.	2.2	120
426	Study of NOx selective catalytic reduction by ethanol over Ag/Al2O3 catalyst on a HD diesel engine. Chemical Engineering Journal, 2008, 135, 195-201.	6.6	45
427	Theoretical and experimental analysis on vibrational spectra of formate species adsorbed on Cu–Al2O3 catalyst. Computational and Theoretical Chemistry, 2008, 857, 38-43.	1.5	15
428	A comparison between the vacuum ultraviolet photoionization time-of-flight mass spectra and the GC/MS total ion chromatograms of polycyclic aromatic hydrocarbons contained in coal soot and multi-component PAH particles. International Journal of Mass Spectrometry, 2008, 274, 64-69.	0.7	18
429	Theoretical and experiment studies on the adsorption of formate species on the surface of catalyst. Journal of Molecular Structure, 2008, 891, 242-246.	1.8	5
430	Characterization and Reactivity of MnO _{<i>x</i>} Supported on Mesoporous Zirconia for Herbicide 2,4-D Mineralization with Ozone. Environmental Science & Technology, 2008, 42, 3363-3368.	4.6	118
431	Novel iron titanate catalyst for the selective catalytic reduction of NO with NH3 in the medium temperature range. Chemical Communications, 2008, , 2043.	2.2	140
432	Heterogeneous reactivity of carbonyl sulfide on α-Al2O3 and γ-Al2O3. Atmospheric Environment, 2008, 42, 960-969.	1.9	35

#	Article	IF	CITATIONS
433	Carbonyls emission from ethanol-blended gasoline and biodiesel-ethanol-diesel used in engines. Atmospheric Environment, 2008, 42, 1349-1358.	1.9	108
434	Combination of biodiesel-ethanol-diesel fuel blend and SCR catalyst assembly to reduce emissions from a heavy-duty diesel engine. Journal of Environmental Sciences, 2008, 20, 177-182.	3.2	51
435	Catalytic Ozonation of Herbicide 2,4-D over Cobalt Oxide Supported on Mesoporous Zirconia. Journal of Physical Chemistry C, 2008, 112, 5978-5983.	1.5	70
436	Selective catalytic reduction of NO by NH3 over a Ce/TiO2 catalyst. Catalysis Communications, 2008, 9, 1453-1457.	1.6	303
437	DFT and DRIFTS Studies on the Adsorption of Acetate on the Ag/Al ₂ O ₃ Catalyst. Journal of Physical Chemistry C, 2008, 112, 6933-6938.	1.5	17
438	Synergistic Effect between NO ₂ and SO ₂ in Their Adsorption and Reaction on γ-Alumina. Journal of Physical Chemistry A, 2008, 112, 6630-6635.	1.1	110
439	Temperature Dependence of the Heterogeneous Reaction of Carbonyl Sulfide on Magnesium Oxide. Journal of Physical Chemistry A, 2008, 112, 2820-2826.	1.1	32
440	Bactericidal Activity of a Ce-Promoted Ag/AlPO4 Catalyst Using Molecular Oxygen in Water. Environmental Science & Technology, 2008, 42, 1699-1704.	4.6	22
441	Catalytic performance of Ag/Al2O3-C2H5OH-Cu/Al2O3 system for the removal of NOx from diesel engine exhaust. Environmental Pollution, 2007, 147, 415-421.	3.7	26
442	Bactericidal Mechanism of Ag/Al ₂ O ₃ against <i>Escherichia coli</i> . Langmuir, 2007, 23, 11197-11199.	1.6	60
443	Oxygen Poisoning Mechanism of Catalytic Hydrolysis of OCS over Al2O3 at Room Temperature. Acta Physico-chimica Sinica, 2007, 23, 997-1002.	0.6	19
444	Mechanism of Heterogeneous Reaction of Carbonyl Sulfide on Magnesium Oxide. Journal of Physical Chemistry A, 2007, 111, 4333-4339.	1.1	36
445	Self-Assembly of Novel Mesoporous Manganese Oxide Nanostructures and Their Application in Oxidative Decomposition of Formaldehyde. Journal of Physical Chemistry C, 2007, 111, 18033-18038.	1.5	248
446	Hydrogen promotes the selective catalytic reduction of NO by ethanol over Ag/Al2O3. Catalysis Communications, 2007, 8, 187-192.	1.6	38
447	A comparative study of TiO2 supported noble metal catalysts for the oxidation of formaldehyde at room temperature. Catalysis Today, 2007, 126, 345-350.	2.2	269
448	Promotion effect of residual K on the decomposition of N2O over cobalt–cerium mixed oxide catalyst. Catalysis Today, 2007, 126, 449-455.	2.2	82
449	An integrated system of biological and catalytic oxidation for the removal of o-xylene from exhaust. Catalysis Today, 2007, 126, 338-344.	2.2	12
450	Catalytic oxidation of nitrogen monoxide over La1â^'xCexCoO3 perovskites. Catalysis Today, 2007, 126, 400-405.	2.2	146

#	Article	IF	CITATIONS
451	Effect of hydrogen on reaction intermediates in the selective catalytic reduction of NOx by C3H6. Applied Catalysis B: Environmental, 2007, 76, 241-247.	10.8	45
452	Catalytic sterilization of Escherichia coli K 12 on Ag/Al2O3 surface. Journal of Inorganic Biochemistry, 2007, 101, 817-823.	1.5	32
453	Uptake and conversion of carbonyl sulfide in a lawn soil. Atmospheric Environment, 2007, 41, 5697-5706.	1.9	4
454	Catalytic decomposition of N2O over CeO2 promoted Co3O4 spinel catalyst. Applied Catalysis B: Environmental, 2007, 75, 167-174.	10.8	439
455	Evidence for the formation, isomerization and decomposition of organo-nitrite and -nitro species during the NOx reduction by C3H6 on Ag/Al2O3. Applied Catalysis B: Environmental, 2007, 75, 298-302.	10.8	26
456	Competitive Reaction During Decomposition of Hexachlorobenzene Over Ultrafine Ca–Fe Composite Oxide Catalyst. Catalysis Letters, 2007, 119, 142-147.	1.4	29
457	Heterogeneous oxidation of carbonyl sulfide on mineral oxides. Science Bulletin, 2007, 52, 2063-2071.	1.7	13
458	Selective catalytic oxidation of ammonia from MAP decomposition. Separation and Purification Technology, 2007, 58, 173-178.	3.9	42
459	Poisoning effect of sulphate on the selective catalytic reduction of NOx by C3H6 over Ag-Pd/Al2O3. Journal of Molecular Catalysis A, 2007, 266, 166-172.	4.8	35
460	Catalytic Decomposition of N ₂ O over Co-M(M=La, Ce, Fe, Mn, Cu, Cr) Composite Oxide Catalysts. Wuli Huaxue Xuebao/ Acta Physico - Chimica Sinica, 2007, 23, 664-670.	2.2	7
461	Disparate effects of SO2 on the selective catalytic reduction of NO by C2H5OH and IPA over Ag/Al2O3. Catalysis Communications, 2006, 7, 657-661.	1.6	9
462	Mechanism of Heterogeneous Oxidation of Carbonyl Sulfide on Al2O3:  An in Situ Diffuse Reflectance Infrared Fourier Transform Spectroscopy Investigation. Journal of Physical Chemistry B, 2006, 110, 3225-3230.	1.2	30
463	Conformational Analysis of Sulfate Species on Ag/Al2O3by Means of Theoretical and Experimental Vibration Spectra. Journal of Physical Chemistry B, 2006, 110, 8320-8324.	1.2	45
464	Study on Effect of SO2 on the Selective Catalytic Reduction of NOx with Propene over Ag/Al2O3 by in Situ DRIFTS. Chinese Journal of Catalysis, 2006, 27, 403-407.	6.9	10
465	Mechanistic Study of Selective Catalytic Reduction of NOx with C2H5OH and CH3OCH3 over Ag/Al2O3 by in Situ DRIFTS. Chinese Journal of Catalysis, 2006, 27, 993-997.	6.9	14
466	Activation of Pt/TiO2 Catalysts by Structural Transformation of Pt-Sites. Catalysis Letters, 2006, 107, 1-4.	1.4	14
467	Significant enhancement of the oxidation of CO by H2 and/or H2O on a FeO x /Pt/TiO2 catalyst. Catalysis Letters, 2006, 110, 185-190.	1.4	56
468	Catalytic performance and mechanism of a Pt/TiO2 catalyst for the oxidation of formaldehyde at room temperature. Applied Catalysis B: Environmental, 2006, 65, 37-43.	10.8	517

#	Article	IF	CITATIONS
469	Emission reduction potential of using ethanol–biodiesel–diesel fuel blend on a heavy-duty diesel engine. Atmospheric Environment, 2006, 40, 2567-2574.	1.9	242
470	Characteristics of carbonyl compounds emission from a diesel-engine using biodiesel–ethanol–diesel as fuel. Atmospheric Environment, 2006, 40, 7057-7065.	1.9	126
471	Effect of SO2 on the performance of Ag-Pd/Al2O3 for the selective catalytic reduction of NOx with C2H5OH. Journal of Environmental Sciences, 2006, 18, 973-978.	3.2	8
472	Conformational analysis and comparison between theoretical and experimental vibration spectra for isocyanate species on Ag/Al2O3 catalyst. Spectrochimica Acta - Part A: Molecular and Biomolecular Spectroscopy, 2005, 61, 1233-1238.	2.0	14
473	Theoretical and experimental study on formation and adsorption of enolic species on Ag-Pd/Al2O3 catalyst. Spectrochimica Acta - Part A: Molecular and Biomolecular Spectroscopy, 2005, 61, 3117-3123.	2.0	5
474	Emission characteristics using methyl soyate?ethanol?diesel fuel blends on a diesel engine. Fuel, 2005, 84, 1543-1543.	3.4	170
475	Selective catalytic reduction of NOx over Ag/Al2O3 catalyst: from reaction mechanism to diesel engine test. Catalysis Today, 2005, 100, 37-47.	2.2	160
476	In situ DRIFTS study of the selective reduction of NOx with alcohols over Ag/Al2O3 catalyst: Role of surface enolic species. Applied Catalysis B: Environmental, 2005, 61, 107-113.	10.8	40
477	Perfect catalytic oxidation of formaldehyde over a Pt/TiO2 catalyst at room temperature. Catalysis Communications, 2005, 6, 211-214.	1.6	216
478	Density Functional Theory (DFT) and DRIFTS Investigations of the Formation and Adsorption of Enolic Species on the Ag/Al2O3Surface. Journal of Physical Chemistry B, 2005, 109, 13291-13295.	1.2	12
479	Heterogeneous Oxidation of Carbonyl Sulfide on Atmospheric Particles and Alumina. Environmental Science & Technology, 2005, 39, 9637-9642.	4.6	33
480	Novel Ag–Pd/Al2O3–SiO2 for lean NO reduction by C3H6 with high tolerance of SO2. Catalysis Communications, 2005, 6, 195-200.	1.6	13
481	Arsenate Adsorption on an Feâ^'Ce Bimetal Oxide Adsorbent:Â Role of Surface Properties. Environmental Science & Technology, 2005, 39, 7246-7253.	4.6	476
482	Elimination of formaldehyde over Cu-Al2O3 catalyst at room temperature. Journal of Environmental Sciences, 2005, 17, 429-32.	3.2	12
483	Removal of azo-dye Acid Red B (ARB) by adsorption and catalytic combustion using magnetic CuFe2O4 powder. Applied Catalysis B: Environmental, 2004, 48, 49-56.	10.8	146
484	Mechanism of the selective catalytic reduction of NOx by C2H5OH over Ag/Al2O3. Applied Catalysis B: Environmental, 2004, 49, 159-171.	10.8	137
485	A New Catalyst for Selective Oxidation of CO in H2: Part 1, Activation by Depositing a Large Amount of FeOxon Pt/Al2O3and Pt/CeO2Catalysts. Catalysis Letters, 2004, 92, 115-121.	1.4	59
486	Selective catalytic reduction of NOx with C3H6 over an Ag/Al2O3 catalyst with a small quantity of noble metal. Catalysis Today, 2004, 93-95, 783-789.	2.2	27

#	Article	IF	CITATIONS
487	FTIR, TPD and DFT studies of intermediates on Ag/Al2O3 during the selective catalytic reduction of NO by C2H5OH. Catalysis Today, 2004, 93-95, 805-809.	2.2	23
488	A comparative study of Ag/Al2O3 and Cu/Al2O3 catalysts for the selective catalytic reduction of NO by C3H6. Catalysis Today, 2004, 90, 191-197.	2.2	70
489	Ozonation of alachlor catalyzed by Cu/Al2O3 in water. Catalysis Today, 2004, 90, 291-296.	2.2	77
490	Selective oxidation of ammonia over copper-silver-based catalysts. Catalysis Today, 2004, 90, 263-267.	2.2	58
491	Catalytic inactivation of SARS coronavirus, Escherichia coli and yeast on solid surface. Catalysis Communications, 2004, 5, 170-172.	1.6	26
492	Preparation and emission characteristics of ethanol-diesel fuel blends. Journal of Environmental Sciences, 2004, 16, 793-6.	3.2	15
493	Adsorption and catalytic combustion of ARB on CuO-Fe2O3. Science Bulletin, 2003, 48, 2311.	1.7	4
494	Novel Pd promoted Ag/Al2O3 catalyst for the selective reduction of NOx. Applied Catalysis B: Environmental, 2003, 46, 365-370.	10.8	55
495	The effect of ethanol blended diesel fuels on emissions from a diesel engine. Atmospheric Environment, 2003, 37, 4965-4971.	1.9	315
496	Novel Enolic Surface Species Formed during Partial Oxidation of CH3CHO, C2H5OH, and C3H6on Ag/Al2O3:Â An in Situ DRIFTS Study. Journal of Physical Chemistry B, 2003, 107, 13090-13092.	1.2	71
497	Photoinduced charge-transfer reaction at surfaces. II. HBrâ< Nan/LiF(001)+hv(610 nm)→Brâ^'Nan+/LiF(001)+H(g). Journal of Chemical Physics, 2003, 119, 9795-980) 1 .2	2
498	Adsorption and thermally induced reactions of halocyclohexanes on a Cu3Pt(111) surface. Surface Science, 2001, 479, 213-223.	0.8	3
499	Self-Limiting Heterogeneous Reactions:Â Bifunctional Hydrocarbon on a Bimetallic Alloy Surface. Journal of Physical Chemistry B, 2000, 104, 12306-12314.	1.2	4
500	Reaction of C60 with oxygen adatoms on Pt(111). Journal of Chemical Physics, 1999, 110, 1173-1179.	1.2	15
501	Polymerization and decomposition ofC60on Pt(111) surfaces. Physical Review B, 1999, 59, 8283-8291.	1.1	42
502	Control of the growth of ordered C 60 films by chemical modification of Pt(111) surfaces. Thin Solid Films, 1999, 348, 30-37.	0.8	17
503	Ordering and stabilization of C 60 films on the (3×3)R30° Sn/Pt(111) surface alloy. Surface Science, 1999, 425, 141-151.	0.8	2
504	Reduction of lean NOx by ethanol over Ag/Al2O3 catalysts in the presence of H2O and SO2. Catalysis Letters, 1998, 50, 87-91.	1.4	104

#	Article	IF	CITATIONS
505	Formation and reactivity of isocyanate (NCO) species on Ag/Al2O3. Journal of the Chemical Society, Faraday Transactions, 1998, 94, 2217-2219.	1.7	93
506	Hydrogenation of carbidic carbon on the Ni(100) surface. Surface Science, 1997, 376, 310-318.	0.8	13
507	Application of highâ€resolution electron energy loss spectroscopy to the adsorption and the photoreaction of CH2I2 and CD3OD on a MoOx thin film. Journal of Vacuum Science and Technology A: Vacuum, Surfaces and Films, 1995, 13, 2689-2697.	0.9	4
508	Oxygen induced direct hydrogenation of CO on Ni(100) surface. Catalysis Letters, 1994, 25, 105-113.	1.4	2
509	Off-normal emission of N2 produced by desorption mediated reaction of NO on Pd(110) surface. Surface Science, 1994, 315, L973-L976.	0.8	28
510	Reduction of CO2with H2O on TiO2(100) and TiO2(110) Single Crystals under UV-irradiation. Chemistry Letters, 1994, 23, 855-858.	0.7	52
511	Formation of CHx species on a Ni(100) surface by the hydrogenation of carbidic carbon. Surface Science, 1993, 283, 117-120.	0.8	10
512	Spectroscopic evidence for the formation of CHx species in the hydrogenation of carbidic carbon on Ni(100). Catalysis Letters, 1992, 16, 407-412.	1.4	12
513	Generation and Release of OH Radicals from the Reaction of H ₂ O with O ₂ over Soot. Angewandte Chemie, 0, , .	1.6	2